Materials Science & Engineering A 828 (2021) 142056

Contents lists available at ScienceDirect

Materials Science & Engineering A

journal homepage: www.elsevier.com/locate/msea

Mechanism-controlled thermomechanical treatment of high manganese steels

Sebastian Wesselmecking [a,*], Marco Haupt [b], Yan Ma [a,c], Wenwen Song [a], Gerhard Hirt [b], Wolfgang Bleck [a]

[a] Steel Institute, RWTH Aachen University, Intzestraße 1, 52072, Aachen, Germany
[b] Institute of Metal Forming, RWTH Aachen University, Intzestraße 10, 52072, Aachen, Germany
[c] Department of Microstructure Physics and Alloy Design, Max-Planck-Institut für Eisenforschung GmbH, Max-Planck-Straße 1, 40237, Düsseldorf, Germany

ARTICLE INFO

Keywords:
High manganese steel
Stacking fault energy
Twinning-induced plasticity
Transformation-induced plasticity
Warm rolling
Recovery annealing

ABSTRACT

Austenitic high manganese steels exhibit outstanding mechanical properties, such as high energy absorption, owing to various deformation-mechanisms such as dislocation slip, twinning-induced plasticity (TWIP) and transformation-induced plasticity (TRIP). Here, we show a novel thermomechanical treatment to manufacture a high manganese steel Fe–18Mn-0.3C (wt.-%) with excellent mechanical performance by combining these three deformation-mechanisms. This process of mechanism-controlled rolling resulted in ultra-high tensile strength of the high manganese steel up to 1.6 GPa, simultaneously with uniform elongations up to 15%.

A thermomechanical process was developed to establish this combination of properties. Warm rolling was conducted at 200 °C, to suppress TRIP and activate TWIP as deformation mechanism. Thus, a high density of deformation twins and dislocations was introduced to the microstructure, avoiding martensite formation. During a subsequent recovery annealing at 520 °C or 550 °C, the dislocation density was reduced, yet the high density of deformation twins was preserved. The combination of warm rolling and recovery annealing resulted in an ultrafine microstructure with a high density of twins and moderate density of dislocations. The TRIP effect is predominant during plastic deformation at ambient conditions in the highly twinned microstructure. The resulting steel exhibits an ultra-high yield strength and sufficient ductility, favorable properties for lightweight construction in automotive or aerospace industry.

1. Introduction

Austenitic high manganese steels, as the main constituent of the second generation of advanced high-strength steels, have attracted immense attention because of their excellent combination of high strength and ductility as well as their high specific energy-absorption capacity [1]. Their outstanding mechanical performance is attributed to additional deformation-mechanisms beside dislocation slip - twinning-induced plasticity (TWIP) and transformation-induced plasticity (TRIP) [2–5]. Both effects, TWIP and TRIP, can result in a high density of crystal defects and substantial microstructure refinement during plastic deformation. TWIP leads to a microstructure refinement, due to the so-called dynamic Hall-Petch effect [6], thus promoting a high work-hardening rate and good ductility [7]. The deformation twins act as effective obstacles to dislocation motion, reducing dislocation mean free path and increasing strength [8,9]. TRIP, the progressive transformation of metastable austenite (face-centered cubic, fcc) to ε-martensite (hexagonal close-packed, hcp) or α'-martensite (body-centered tetragonal, bct) during plastic deformation, is able to retard strain localization and facilitate homogeneous deformation [10,11]. Especially, ε-martensite is considered to be a strong barrier to dislocation movement, due to its hcp structure [12]. Thus, the TRIP effect improves work-hardening rate and ductility significantly [13,14].

The TWIP and TRIP effects can occur simultaneously or individually, which is closely related to stacking fault energy (SFE) of austenite. Such an intrinsic material's parameter depends on chemical composition, temperature, and stress state [15–18]. Generally, a low SFE (<20 mJ/m^2) enables the TRIP effect, a higher SFE (~20–50 mJ/m^2) results in the TWIP effect. Both deformation-mechanisms can occur at the same time, when the SFE is within a transition area [19–23]. Due to the dependence of SFE on temperature, the deformation-mechanisms and mechanical properties can be altered readily by adjusting deformation

* Corresponding author.
E-mail address: sebastian.wesselmecking@rwth-aachen.de (S. Wesselmecking).

https://doi.org/10.1016/j.msea.2021.142056
Received 17 May 2021; Received in revised form 9 August 2021; Accepted 10 September 2021
Available online 20 September 2021

Table 1
Chemical composition of the Fe–18Mn-0.3C steel and the stacking fault energy (SFE) at room temperature (RT) and 200 °C.

C	Mn	Al	Si	S	N	SFE	SFE
wt.-% 0.32	wt.-% 18.6	ppm <10	wt.-% 0.03	ppm 76	ppm 21	at RT 12 mJ/m^2	at 200 °C 46 mJ/m^2

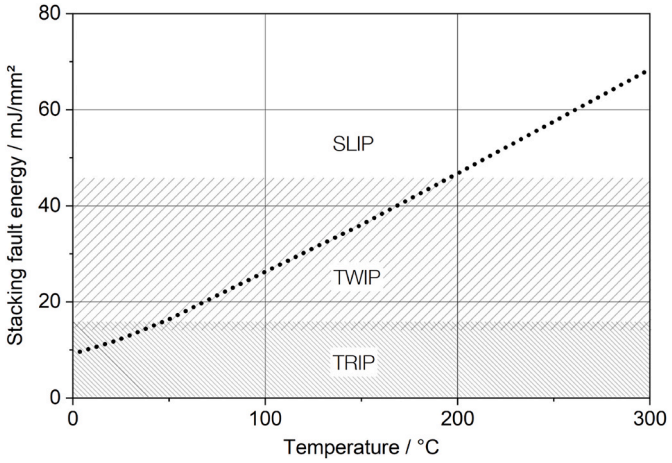

Fig. 1. Development of SFE from 0 °C to 300 °C and estimated deformation mechanism during tensile testing [35,36].

temperature [24].

Despite outstanding work-hardening behavior, high manganese steels often show low yield strength because of the soft austenitic matrix [25]. Nevertheless, high yield strength is strongly demanded for safety-related components. Versatile efforts have been made to enhance the yield strength of high manganese steels, such as solid-solution strengthening, precipitation strengthening, and dislocation strengthening [26–30]. Such strengthening strategies often retain the strength-ductility trade-off, unfortunately leading to a decline in formability. Whereas, grain refinement is known to improve strength without sacrificing ductility. In high manganese steels, such a strengthening effect can be realized by reducing austenite grain size and introducing twin boundaries. Recent studies revealed that recovery annealing is a promising way in TWIP steels, preserving a high density of deformation twins while reducing dislocation density after cold rolling [31,32]. Such a recovered microstructure possesses high yield strength but rather low uniform elongation. The low uniform elongation is a consequence of the limited strain hardening. This in turn is the result of the reduced twinning rate at high strain levels [33].

In the present study, we developed a novel thermomechanical treatment, combining deformation-mechanism-controlled rolling and recovery annealing to further optimize the mechanical performance of high manganese steels. This engineering strategy is based on utilization of temperature dependence of the SFE and thus deformation-mechanisms. We designed a high manganese steel, in which the TRIP effect is predominant at room temperature. The TWIP effect dominates during warm rolling as temperature determines the deformation mechanism. This mechanism-controlled rolling results in a highly twinned microstructure. Subsequent recovery annealing reduces dislocation density yet preserves the beneficial deformation twins. The microstructure evolution during the thermomechanical treatment and following tensile deformation is analyzed. The impact of microstructure on mechanical properties is discussed.

2. Materials and methods

A high manganese steel with the nominal chemical composition of Fe–18Mn-0.3C (wt.-%) was investigated. The attained chemical composition, determined by wet chemical analysis, is given in Table 1.

The SFE was estimated using a thermodynamic subregular solution model [34]. SFE development within a range from 0°C to 300 °C is given in Fig. 1. At room temperature, the SFE is ~12 mJ/m^2 and thus the TRIP effect is expected to prevail during tensile tests [35,36]. The SFE increases to ~46 mJ/m^2 at 200 °C. Similar investigations on HMnS with higher SFE have shown twinning during rolling up to temperatures of 400 °C [37,38].

The laboratory processing of the samples is shown in Fig. 2. The steel was produced in a vacuum induction furnace followed by ingot casting. The steel was forged at 1150 °C from 140 mm × 140 mm–160 mm × 60 mm and then homogenized for 5 h at 1150 °C. After homogenization, hot rolling was conducted at 1150 °C to reduce the sheet thickness to 3 mm. For subsequent warm rolling, the sheets were heated up to the target temperature in an air circulation furnace. The warm rolling was performed at 200 °C in 6–7 rolling passes until a thickness reduction of 50% (1.5 mm) was achieved. The temperature-loss during transportation from furnace to rolling mill was 15 °C, which was determined by infrared thermography. The temperature loss was compensated by increased furnace temperature. The temperature loss due to contact with the rolling mill was not compensated, expecting a small temperature loss during rolling and a SFE within TWIP range (Fig. 1).

Tensile test samples were manufactured perpendicular to the rolling direction by water jet cutting and subjected to recovery annealing. Recovery annealing was conducted in a salt bath furnace using salt GS430 with an inhibitor to avoid surface depletion of carbon. The mechanical properties were evaluated by tensile tests at room temperature at strain rate of 0.001 s^{-1} according to the standard DIN EN ISO 6892 in a Zwick Z250 machine. The gauge length and width of the tensile samples were

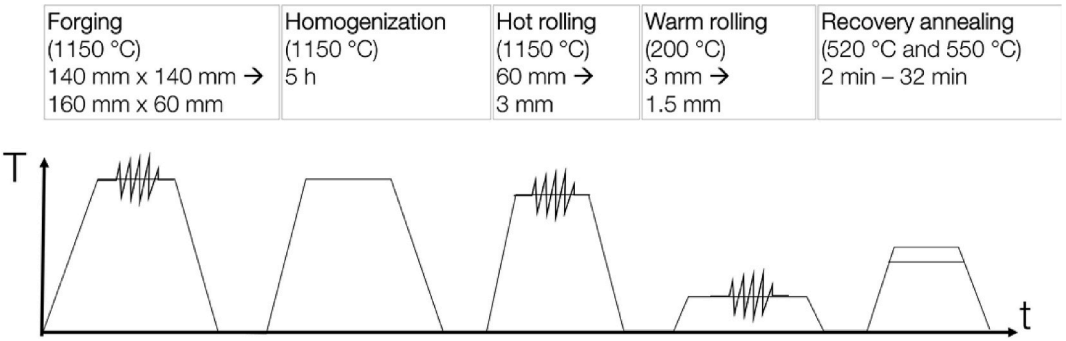

Fig. 2. *Laboratory process chain of the investigated* Fe–18Mn-0.3C.

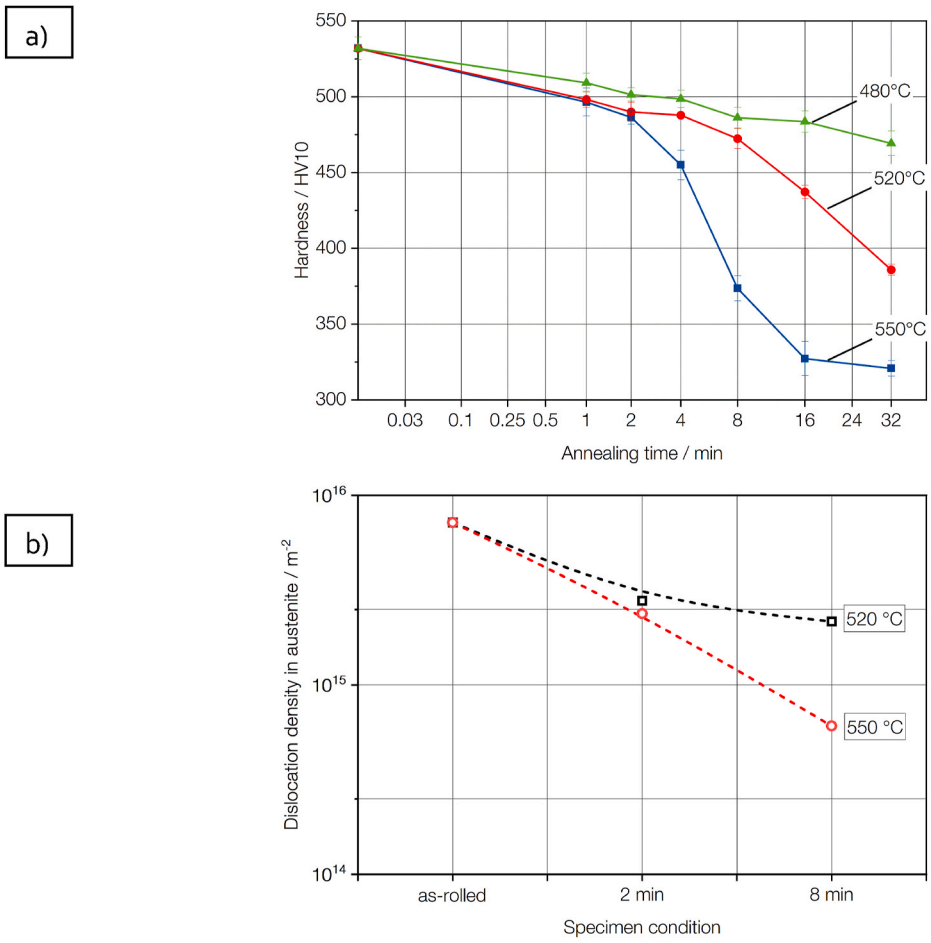

Fig. 3. a) Hardness evolution (HV10) of warm-rolled material upon recovery annealing at 480 °C, 520 °C and 550 °C for up to 32 min. b) Development of dislocation density from HEXRD peak analysis.

30 mm and 6 mm, respectively. A Zwick multiXtens system was employed for a strain measurement (accuracy class 0.5). To identify promising process windows for recovery annealing, hardness measurements (HV10 - DIN EN ISO 14577) were carried out to evaluate the softening degree [39].

The microstructure was characterized from the cross section of tensile samples. The surface was prepared by mechanical grinding with SiC grinding paper down to 4000 grit and followed by polishing with 3 µm, 1 µm and 0.25 µm diamond suspension, finalized by electro-polishing. Electron backscatter diffraction (EBSD) measurements were performed using a JEOL JSM 7000 F equipped with an EDAX Hikari detector. The acceleration voltage of the electron beam was 20 kV and the step size was 0.20 µm. Sigma 3 twin boundaries are indexed in the EBSD images within a orientation misfit of ±3°. Moreover, synchrotron high-energy X-ray diffraction (HEXRD) was conducted at beamline P02.1 [40] of PETRA III at Deutsches Elektronen-Synchrotron (DESY) to quantify the phases and dislocation density of austenite. The wavelength of the monochromatic X-ray beam was ~0.207 Å. Debye-Scherrer rings were recorded by a PerkinElmer XRD1621 area detector. The beam size was 0.6 mm × 0.6 mm. The exposure time for one measurement was 10 s. The diffraction profiles were analyzed by the Rietveld refinement method using the MAUD software and the detailed procedures were documented elsewhere [41]. The XRD peaks indicate the imperfections of materials and in particular the peak broadening is strongly affected by microstrain and crystallite size. Dislocations as major crystal defects significantly contribute to microstrain [42]. The Popa model [43] integrated into the Rietveld Refinement software MAUD was used to calculate crystallite size and microstrain for austenite. These values were used as input to calculate the dislocation density by the Williamson-Smallman equation [44].

$$\rho = \frac{3\sqrt{2\pi}\left(\varepsilon^2\right)^{1/2}}{Db}. \quad (1)$$

$\left(\varepsilon^2\right)^{1/2}$ is the average microstrain, D is the average crystallite size, and b is the Burgers vector. The instrument broadening was subtracted for each measurement, which was measured using a standard sample CeO2. The dislocation evolution qualitatively describes the reduction of dislocation density during annealing within the austenite phase.

3. Results

The warm-rolled high manganese steel revealed an austenitic microstructure as confirmed by the HEXRD measurement. The dislocation density in austenite was about 7.2 × 10^{15} m^{-2}. The as-rolled material was annealed at 480 °C, 520 °C and 550 °C for up to 32 min. As shown in Fig. 3 a), the hardness decreased with an increase in annealing temperature and time. The hardness drastically declined after annealing for 8 min at 520 °C (red line) and 4 min 550 °C (blue line), respectively.

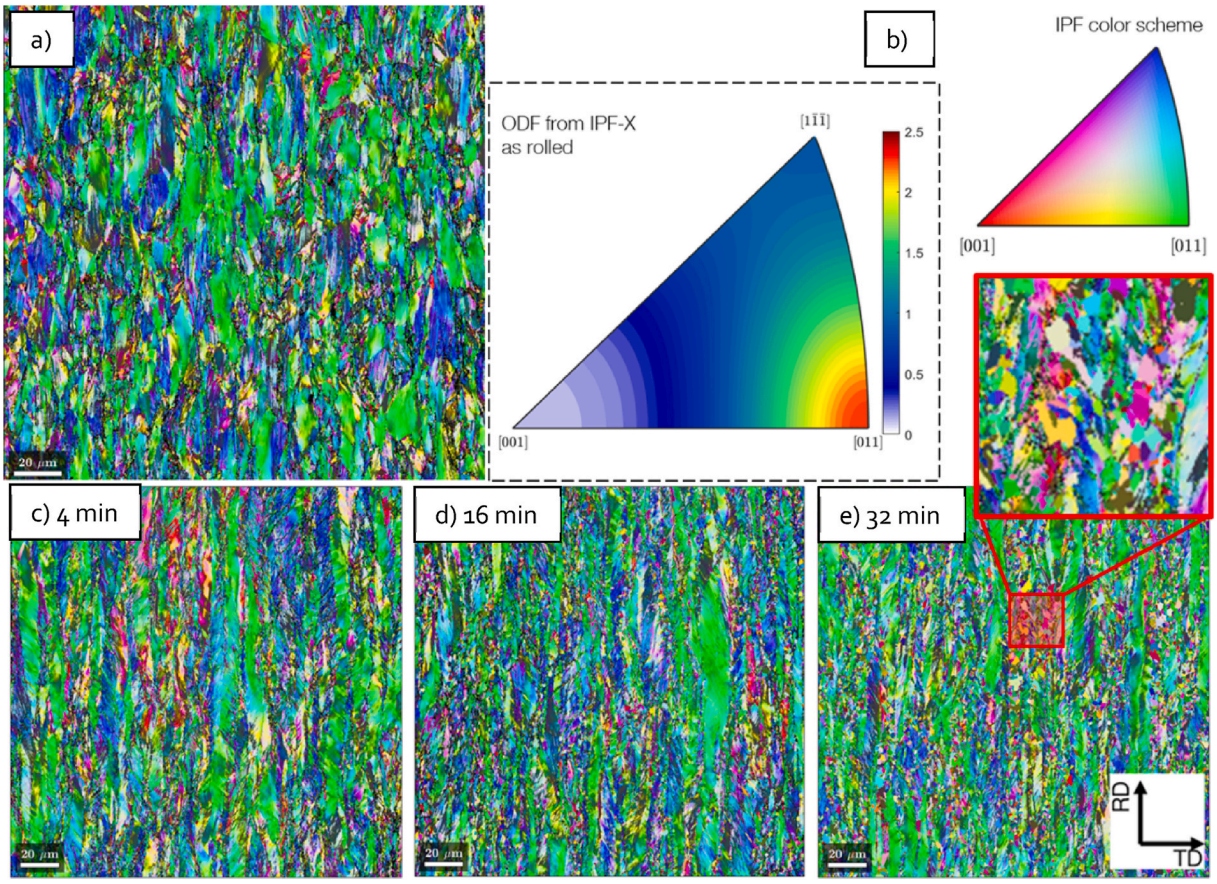

Fig. 4. EBSD IPF maps of the Fe–18Mn-0.3C steel (a) after warm rolling at 200°C and after recovery annealing at 520 °C for (c) 4 min, (d) 16 min, and (e) 32 min with a magnified illustration of the already recrystallized grains. b) depicts the ODF from the given EBSD IPF-X map. Unassignable points are depicted as black.

Annealing at 480 °C led to slow kinetics, thus was not further investigated. The HEXRD results also indicated a subtle decrease in dislocation density in the specimen annealed at 520 °C for up to 8 min. However, the dislocation density was significantly reduced in the specimen annealed at 550 °C for 8 min to 0.6×10^{15} m^{-2} (Fig. 3 b)).

The strong decrease in hardness and dislocation density indicated the occurrence of recrystallization [45], which is expected at temperatures above approx. 500 °C [46] especially in highly deformed regions [47]. The microstructural development was evaluated by EBSD measurements, as shown in Fig. 4**.** The EBSD IPF figures show elongated grains after rolling. After 16 min d) and 32 min e) heat treatment small recrystallized grains are visible, as shown in the magnification (red square). The recrystallized grains have significantly lower KAM values, and are, for better recognition, depicted in Fig. 5. The ODF from Fig. 5 a) is given in Fig. 5 b) and indicates the alignment of the grains after rolling.

To depict recrystallization a threshold of the kernel average misorientation (KAM) was set to 0.45. Fig. 5 b) depicts the KAM distribution function for all conditions. After 16 min (yellow) and 32 min (red) recrystallized areas with significant lower KAM-values are formed. The related KAM microstructures are depicted (a), c), d) and e)) and the recrystallized (RX) microstructure is highlighted in blue color. After rolling the detectable sigma 3 twin boundaries are visible (red lines) in Fig. 5 a). Twins are depicted as well after annealing for 4 min in Fig. 5 c), showing a high twin density for both states. After annealing at 520 °C for 4 min (Fig. 5 b)), only recovery and yet no RX was observed. Partial recrystallization (8%) occurred after 16 min (Fig. 5 c)). The recrystallization degree further increased to 22.5% RX after annealing for 32 min (Fig. 5 d)).

According to the hardness tests and microstructure characterization, tensile properties were further evaluated of the material annealed at 520 °C and 550 °C for 2 min, 4 min, and 8 min, as depicted in Fig. 6 a)**.** The as-rolled steel (dashed black line) revealed very high ultimate tensile strength (UTS) of 1867 MPa, albeit very limited total elongation (TE). The recovery annealing resulted in an excellent combination of high strength and superior ductility. The steel annealed at 520 °C for 2 min showed UTS of 1636 MPa with TE of 14.8%. With an increase in annealing time to 4 min, the UTS slightly declined to 1558 MPa, while TE increased to 18.7%. Annealing at 550 °C led to a more rapid change in mechanical properties, but the trend was the same as the steel annealed at 520 °C. UTS of the steel annealed at 550 °C for 2 min was 1550 MPa, decreasing to 1450 MPa and 1308 MPa after annealing for 4 min and 8 min, respectively. Total elongation raised from 17.5% (2 min) to 41.7% (8 min). Strain hardening and true stress-strain curves are shown in Fig. 6 b). It is worth pointing out that the specimens annealed in different conditions (520°C/8 min; 550 °C/2 min) possessed a similar true strength level (~1750 MPa), however, they showed different uniform elongation. Obviously, an increase in annealing temperature and time enhanced the strain-hardening rate and postponed necking of the steel, thus resulting in better ductility. The HEXRD measurements

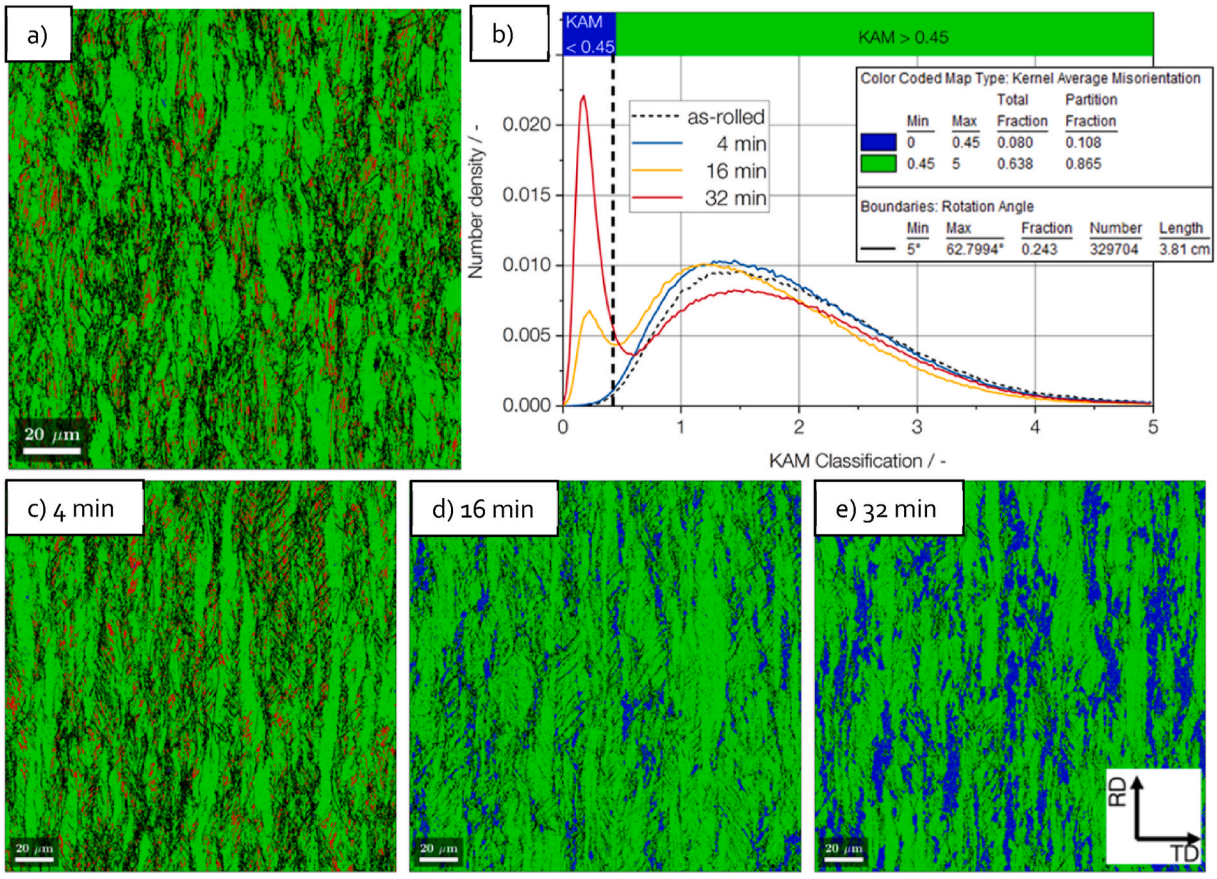

Fig. 5. EBSD kernel average misorientation maps (a) after warm rolling at 200°C with sigma 3 twin boundaries in red, and after recovery annealing at 520 °C for (c) 4 min with sigma 3 twin boundaries in red, (d) 16 min, and (e) 32 min (Grains considered recrystallized (KAM classification <0.45) are depicted in dark blue). KAM distribution functions for the given figures are given in b). (For interpretation of the references to color in this figure legend, the reader is referred to the Web version of this article.)

indicated that austenite readily transformed into ε-martensite during deformation in all samples (Fig. 6 c)). For the specimen annealed at 550 °C for 8 min, about 4 vol.-% α'-martensite was also observed after straining.

4. Discussion

Recovery annealing after warm rolling of high manganese steels results in high yield strength, as reported in [48]. A disadvantage of the concept is the low uniform elongation, due to limited work hardening. The work hardening capacity of ultrafine grained or highly twinned microstructures is low and accommodation of dislocations is limited [49,50]. To overcome this limitation and improve industrial feasibility, we designed an alternative thermomechanical treatment. The decisive advancement here is to utilize the TRIP effect in the recovery annealed and highly twinned microstructure to improve the work hardening behavior. Such a strategy enables the combination of the TWIP and TRIP effects in individual manufacturing processes to optimize the mechanical performance of high manganese steels (Fig. 7).

In order to determine the process window for recovery annealing, we first examined temperature and time for the recrystallization start. Hardness evolution of warm rolled samples showed that low recovery annealing temperature postpones the onset of recrystallization to 2 min and 8 min annealing time at 550 °C and 520 °C, respectively. This could also be monitored by Synchrotron measurement as a strong reduction of peak width correlates with the onset of recrystallization.

After recovery annealing all samples were fully austenitic. During plastic deformation at room temperature, the TRIP effect was observed as predominant deformation mechanism, which results in pronounced strain hardening. ε-martensite develops due to deformation and behaves like a hard obstacle for dislocation movement [12] in the highly twinned microstructure. The highest yield strength of 1600 MPa has been obtained after only 2 min annealing at 520°C. The highest total elongation of ~40% was gained with a yield strength of 1000 MPa when partial recrystallization was accepted due to annealing at 550°C for 8 min. However, this high total elongation comes along with the occurrence of serrated flow, obviously as a consequence of partial recrystallization [51].

The mechanical properties of steel processed by this thermomechanical treatment outperform other concepts for ultra-high-strength cold formable steels. The new process can be divided into 3 steps.

Mechanism-controlled rolling: The SFE of the Fe–18Mn-0.3C is originally 12 mJ/mm^2 at RT, thus deformation is supposed to be predominated by the TRIP effect. To manipulate the microstructure and introduce twins, rolling can be conducted at an elevated temperature (here 200 °C, SFE 46 mJ/m^2). Such deformation-mechanism-controlled

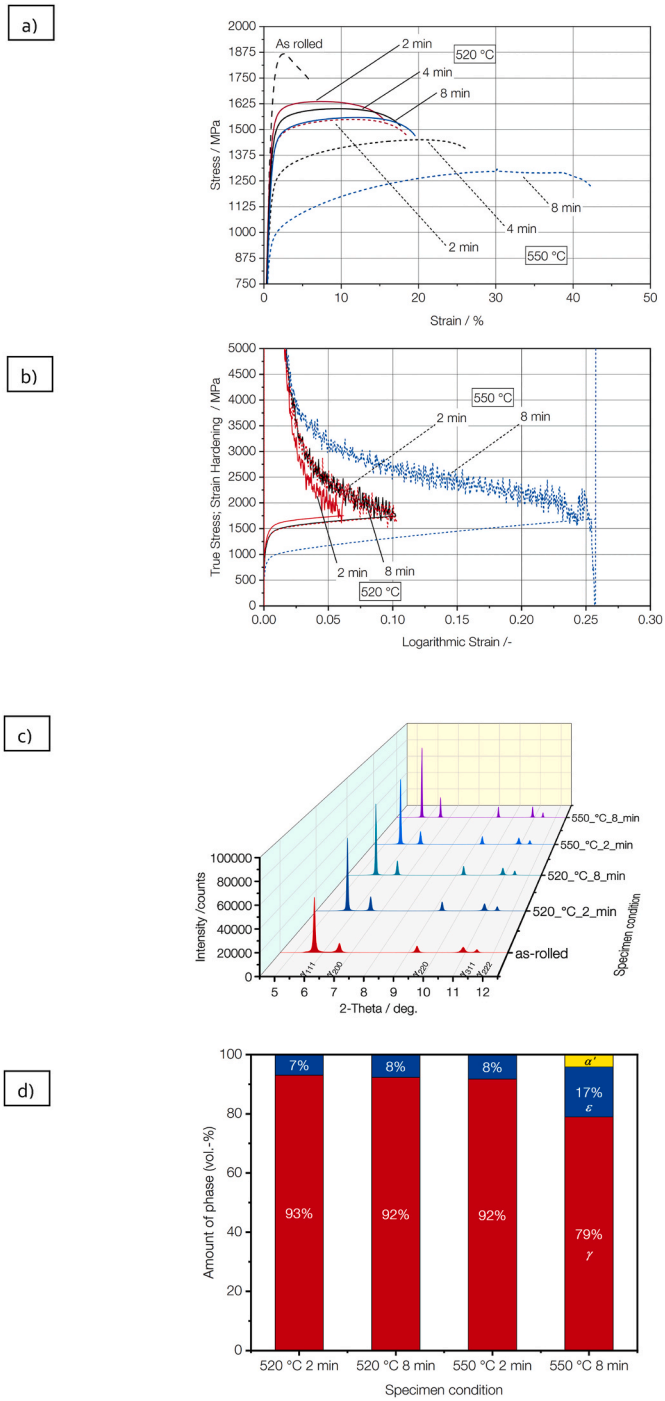

Fig. 6. a) Engineering stress-strain curves of the high manganese steel after recovery annealing at 520 °C and 550 °C for different annealing times; b) True stress-strain curves and strain hardening-strain curves. c) HEXRD-spectra and d) HEXRD-phase analysis of the investigated samples.

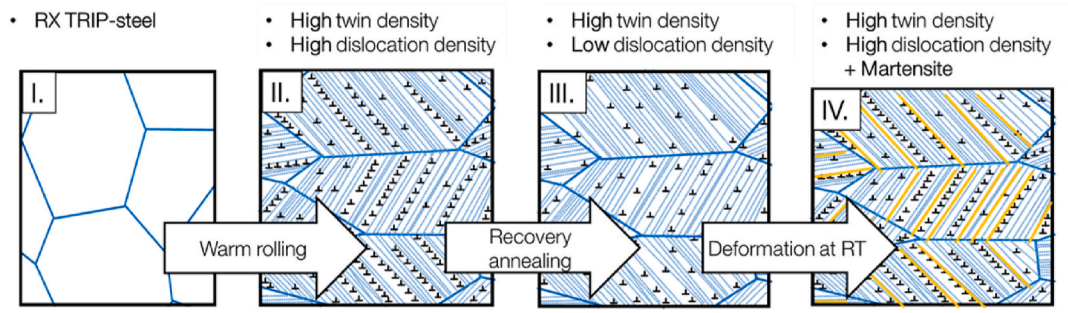

Fig. 7. Schematic illustration of the microstructure evolution during the thermomechanical treatment and cold deformation.

rolling results in a high density of dislocations and deformation twins.

Recovery Annealing: To reestablish cold formability, recovery annealing is employed to reduce dislocation density. In this stage, however, deformation twins should be preserved. Thus, recrystallization and high annealing temperatures must be avoided.

Deformation at room temperature: Because of the highly twinned microstructure, the onset of plastic deformation is strongly impeded which results in the ultra-high yield strength of 1.6 GPa. Due to the low SFE of the steel at room temperature, the TRIP effect plays an important role during cold forming. The austenite to martensite transformation retards strain localization and promotes a high work-hardening rate. As a result, the steel shows an excellent combination of high strength and superior ductility.

The present study demonstrates the successful approach for processing and property optimization based on the temperature-dependent deformation-mechanisms in high manganese steels. The thermomechanical treatment consists of a **mechanism-controlled rolling** and a subsequent **recovery annealing**. Mechanism-controlled rolling produced a highly deformed austenite with a high density of dislocations and deformation twins. Recovery annealing reduced the dislocation density to recover the cold formability, preserving deformation twins. Such a highly twinned microstructure substantially enhanced the yield strength of austenitic high manganese steels. The TRIP effect during tensile deformation promotes an increased strain-hardening rate and thus reduces localization of strain [52,53].

The mechanical properties of steel processed by the new processing strategy show beneficial mechanical properties compared to other excellent concepts for ultra-high-strength steels. The comparison of the engineering stress-engineering strain curves of several steels in Fig. 8 indicate the prolonged uniform elongation range of the warm rolled material, compared to the concept of a newly developed ultra-fast cooled dual phase steel [54] and especially compared to a recovery annealed TWIP-steel with a highly twinned microstructure with higher SFE during straining [48]. The proposed mechanism-controlled rolling provides a new way to manufacture high manganese steels with excellent properties.

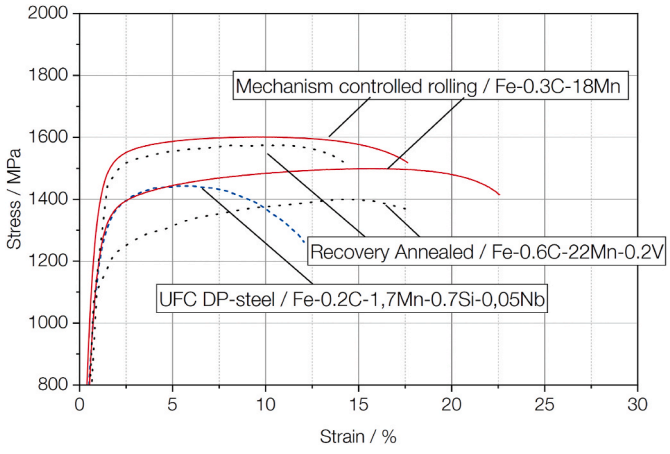

Fig. 8. Engineering stress strain curves of the warm rolled steel compared with other ultra-high strength steels [48,54]. (UFC – ultra fast cooled; DP – dual phase).

5. Summary and conclusions

A new processing, consisting of warm rolling and subsequent recovery annealing, was presented and the influence of changes in processing parameters was investigated. Our aim, to activate the TRIP effect in a twinned and recovery annealed microstructure, was successfully accomplished during tensile tests. The following conclusions can be drawn.

- The suppression of martensite formation during rolling was accomplished by control of stacking fault energy during warm rolling. The increased stacking fault energy led to twin formation. EBSD measurements conducted on the as-rolled microstructure revealed twins but determination of twin density by EBSD is rather vague. Therefore, we would recommend further high-resolution measurements to describe the evolution of the twin density as a function of the process parameters, and thus provide a detailed picture on the microstructural evolution and mechanical properties.
- Recovery annealing, used to reduce the dislocation density after rolling, retained the twinned microstructure of the warm-rolled steel. Applied hardness measurements were successfully used to determine onset of recrystallization, which was proven by HEXRD. This is a simple way to prevent recrystallization and to achieve homogeneous mechanical properties avoiding partial recrystallization.
- Using the new proposed processing route led to excellent mechanical properties of more than 1.6 GPa yield strength and more than 15% uniform elongation. Since the rolling structure is essentially preserved and only dislocation degradation takes place, strongly anisotropic properties can be assumed, which should be investigated further. In addition, the description of the microstructure after rolling, in particular the martensite development in the structure, is challenging. This will be the focus of further work.

Data availability

The data supporting the findings of this study are available from the corresponding authors upon request.

CRediT authorship contribution statement

Sebastian Wesselmecking: Conceptualization, Investigation, Formal analysis, Methodology, Writing – original draft. **Marco Haupt:** Investigation, Writing – review & editing. **Yan Ma:** Visualization, Formal analysis, Writing – review & editing. **Wenwen Song:** Writing – review & editing. **Gerhard Hirt:** Writing – review & editing, Supervision. **Wolfgang Bleck:** Writing – review & editing, Supervision.

Declaration of competing interest

The authors declare that they have no known competing financial interests or personal relationships that could have appeared to influence the work reported in this paper.

Acknowledgement

The authors gratefully acknowledge the financial support of the DFG (Deutsche Forschungsgemeinschaft) within the collaborative research center SFB 761 “steel – ab initio”. The synchrotron high-energy X-ray diffraction measurements were carried out at the Powder Diffraction and Total Scattering Beamline P02.1 of PETRA III at DESY (Proposal No.: I-20181007), a member of the Helmholtz Association (HGF), which is gratefully acknowledged.

References

[1] B.C. de Cooman, L. Chen, H.S. Kim, Y. Estrin, S.K. Kim, H. Voswinckel, State-of-the-Science of high manganese TWIP steels for automotive applications, in: A. Haldar, S. Suwas, D. Bhattacharjee (Eds.), Microstructure and Texture in Steels, Springer London, London, 2009, pp. 165–183.
[2] W.S. Choi, S. Sandlöbes, N.V. Malyar, C. Kirchlechner, S. Korte-Kerzel, G. Dehm, P.-P. Choi, D. Raabe, On the nature of twin boundary-associated strengthening in Fe-Mn-C steel, Scripta Mater. 156 (2018) 27–31, https://doi.org/10.1016/j.scriptamat.2018.07.009.
[3] W.S. Choi, S. Sandlöbes, N.V. Malyar, C. Kirchlechner, S. Korte-Kerzel, G. Dehm, B. C. de Cooman, D. Raabe, Dislocation interaction and twinning-induced plasticity in face-centered cubic Fe-Mn-C micro-pillars, Acta Mater. 132 (2017) 162–173, https://doi.org/10.1016/j.actamat.2017.04.043.
[4] O. Grässel, G. Frommeyer, C. Derder, H. Hofmann, Phase transformations and mechanical properties of Fe-Mn-Si-Al TRIP-steels, 07, J. Phys. IV France (1997) C5–C383, https://doi.org/10.1051/jp4:1997560. C5-388.
[5] U. Brüx, G. Frommeyer, O. Grässel, L.W. Meyer, A. Weise, Development and characterization of high strength impact resistant Fe-Mn-(Al-, Si) TRIP/TWIP steels, Steel Res. 73 (2002) 294–298, https://doi.org/10.1002/srin.200200211.
[6] F. de las Cuevas, M. Reis, A. Ferraiuolo, G. Pratolongo, L.P. Karjalainen, J. Alkorta, J. Gil Sevillano, Hall-petch relationship of a TWIP steel, KEM 423 (2009) 147–152. https://doi.org/10.4028/www.scientific.net/KEM.423.147.
[7] S. Allain, J.-P. Chateau, O. Bouaziz, Constitutive model of the TWIP effect in a polycrystalline high manganese content austenitic steel, Steel Res. 73 (2002) 299–302, https://doi.org/10.1002/srin.200200212.
[8] O. Bouaziz, S. Allain, C. Scott, Effect of grain and twin boundaries on the hardening mechanisms of twinning-induced plasticity steels, Scripta Mater. 58 (2008) 484–487, https://doi.org/10.1016/j.scriptamat.2007.10.050.
[9] O. Bouaziz, N. Guelton, Modelling of TWIP effect on work-hardening, 319-321, Materials Science and Engineering: A (2001) 246–249, https://doi.org/10.1016/S0921-5093(00)02019-0.
[10] A. Bogers, W. Burgers, Partial dislocations on the {110} planes in the B.C.C. lattice and the transition of the F.C.C. into the B.C.C. lattice, Acta Metall. 12 (1964) 255–261.
[11] G.B. Olson, M. Cohen, A general mechanism of martensitic nucleation: Part I. General concepts and the FCC → HCP transformation, MTA 7 (1976) 1897–1904, https://doi.org/10.1007/BF02659822.
[12] Y. Tomota, M. Strum, J.W. Morris, Microstructural dependence of Fe-high Mn tensile behavior, MTA 17 (1986) 537–547, https://doi.org/10.1007/BF02643961.
[13] M. Koyama, T. Sawaguchi, T. Lee, C.S. Lee, K. Tsuzaki, Work hardening associated with ϵ-martensitic transformation, deformation twinning and dynamic strain aging in Fe–17Mn–0.6C and Fe–17Mn–0.8C TWIP steels, Materials Science and Engineering: A 528 (2011) 7310–7316, https://doi.org/10.1016/j.msea.2011.06.011.
[14] D. Cornette, T. Hourman, O. Hudin, J.P. Laurent, A. Reynaert, High Strength Steels for Automotive Safety Parts. https://doi.org/10.4271/2001-01-0078.
[15] W. Bleck, X. Guo, Y. Ma, The TRIP effect and its application in cold formable sheet steels, steel research int 88 (2017) 1700218, https://doi.org/10.1002/srin.201700218.
[16] D.T. Pierce, J.A. Jiménez, J. Bentley, D. Raabe, J.E. Wittig, The influence of stacking fault energy on the microstructural and strain-hardening evolution of Fe–Mn–Al–Si steels during tensile deformation, Acta Mater. 100 (2015) 178–190, https://doi.org/10.1016/j.actamat.2015.08.030.
[17] J.-K. Kim, B.C. de Cooman, Stacking fault energy and deformation mechanisms in Fe-xMn-0.6C-yAl TWIP steel, Mater. Sci. Eng. 676 (2016) 216–231, https://doi.org/10.1016/j.msea.2016.08.106.
[18] H. Ding, H. Ding, C. Qiu, Z. Tang, J. Zeng, P. Yang, Formability of TRIP/TWIP steel containing manganese of 18.8%, Journal of Iron and Steel Research, International 18 (2011) 36–40, https://doi.org/10.1016/S1006-706X(11)60008-3.
[19] H. Ding, H. Ding, D. Song, Z. Tang, P. Yang, Strain hardening behavior of a TRIP/TWIP steel with 18.8% Mn, Materials Science and Engineering: A 528 (2011) 868–873, https://doi.org/10.1016/j.msea.2010.10.040.
[20] X. Guo, Influences of Microstructure, Alloying Elements and Forming Parameters on Delayed Fracture in TRIP/TWIP-aided Austenitic Steels: Dissertation, Shaker, Aachen, 2012.
[21] B. Hu, B. He, G. Cheng, H. Yen, M. Huang, H. Luo, Super-high-strength and formable medium Mn steel manufactured by warm rolling process, Acta Mater. 174 (2019) 131–141, https://doi.org/10.1016/j.actamat.2019.05.043.
[22] J.J. Du, X. Zhang, B.X. Liu, Y.C. Dong, J.H. Feng, C.X. Chen, F.X. Yin, Interface strengthening and fracture behavior of multilayer TWIP/TRIP steel, Mater. Chem. Phys. 223 (2019) 114–121, https://doi.org/10.1016/j.matchemphys.2018.10.051.
[23] T. Hickel, S. Sandlöbes, R. Marceau, A. Dick, I. Bleskov, J. Neugebauer, D. Raabe, Impact of nanodiffusion on the stacking fault energy in high-strength steels, Acta Mater. 75 (2014) 147–155, https://doi.org/10.1016/j.actamat.2014.04.062.
[24] A. Asghari, A. Zarei-Hanzaki, M. Eskandari, Temperature dependence of plastic deformation mechanisms in a modified transformation-twinning induced plasticity steel, Materials Science and Engineering: A 579 (2013) 150–156, https://doi.org/10.1016/j.msea.2013.04.106.
[25] G. Yang, J.-K. Kim, An overview of high yield strength twinning-induced plasticity steels, Metals 11 (2021) 124, https://doi.org/10.3390/met11010124.
[26] H. Gwon, J.-K. Kim, S. Shin, L. Cho, B.C. de Cooman, The effect of vanadium micro-alloying on the microstructure and the tensile behavior of TWIP steel, Materials Science and Engineering: A 696 (2017) 416–428, https://doi.org/10.1016/j.msea.2017.04.083.
[27] P. Kusakin, A. Belyakov, D.A. Molodov, R. Kaibyshev, On the effect of chemical composition on yield strength of TWIP steels, Materials Science and Engineering: A 687 (2017) 82–84, https://doi.org/10.1016/j.msea.2017.01.080.
[28] M. Klimova, S. Zherebtsov, N. Stepanov, G. Salishchev, C. Haase, D.A. Molodov, Microstructure and texture evolution of a high manganese TWIP steel during cryo-rolling, Mater. Char. 132 (2017) 20–30, https://doi.org/10.1016/j.matchar.2017.07.043.
[29] T. Allam, X. Guo, S. Sevsek, M. Lipińska-Chwałek, A. Hamada, E. Ahmed, W. Bleck, Development of a Cr-Ni-V-N medium manganese steel with balanced mechanical and corrosion properties, Metals 9 (2019) 705, https://doi.org/10.3390/met9060705.
[30] S. Wesselmecking, W. Song, Y. Ma, T. Roesler, H. Hofmann, W. Bleck, Strain aging behavior of an austenitic high-Mn steel, steel research int 89 (2018) 1700515, https://doi.org/10.1002/srin.201700515.
[31] S. Allain, O. Bouaziz, J.P. Chateau, Thermally activated dislocation dynamics in austenitic FeMnC steels at low homologous temperature, Scripta Mater. 62 (2010) 500–503, https://doi.org/10.1016/j.scriptamat.2009.12.026.
[32] C. Haase, Texture and Microstructure Evolution during Deformation and Annealing of HMnS TWIP Steels, Dissertation, Aachen, 2015.
[33] D.R. Steinmetz, T. Jäpel, B. Wietbrock, P. Eisenlohr, I. Gutierrez-Urrutia, A. Saeed–Akbari, T. Hickel, F. Roters, D. Raabe, Revealing the strain-hardening behavior of twinning-induced plasticity steels: theory, simulations, experiments, Acta Mater. 61 (2013) 494–510, https://doi.org/10.1016/j.actamat.2012.09.064.
[34] A. Saeed-Akbari, L. Mosecker, A. Schwedt, W. Bleck, Characterization and prediction of flow behavior in high-manganese twinning induced plasticity steels: Part I. Mechanism maps and work-hardening behavior, Metall and Mat Trans A 43 (2012) 1688–1704, https://doi.org/10.1007/s11661-011-0993-4.
[35] L. Remy, Kinetics of strain-induced fcc→hcp martensitic transformation, MTA 8 (1977) 253–258, https://doi.org/10.1007/BF02661637.
[36] L. Rémy, The interaction between slip and twinning systems and the influence of twinning on the mechanical behavior of fcc metals and alloys, MTA 12 (1981) 387–408, https://doi.org/10.1007/BF02648536.
[37] Müller Haupt, Haase, Sevsek, Schwedt Brasche, Hirt, The influence of warm rolling on microstructure and deformation behavior of high manganese steels, Metals 9 (2019) 797, https://doi.org/10.3390/met9070797.
[38] B.C. de Cooman, High Mn TWIP steel and medium Mn steel, in: R. Rana, S.B. Singh (Eds.), Automotive Steels: Design, Metallurgy, Processing and Applications, Woodhead Publishing, Duxford, 2017, pp. 317–385.
[39] G. Gottstein, Materialwissenschaft und Werkstofftechnik: Physikalische Grundlagen, fourth ed., Springer Vieweg, Berlin u.a., 2014.
[40] A.-C. Dippel, H.-P. Liermann, J.T. Delitz, P. Walter, H. Schulte-Schrepping, O. H. Seeck, H. Franz, Beamline P02.1 at PETRA III for high-resolution and high-energy powder diffraction, J. Synchrotron Radiat. 22 (2015) 675–687, https://doi.org/10.1107/S1600577515002222.
[41] Y. Ma, W. Song, W. Bleck, Investigation of the microstructure evolution in a Fe-17Mn-1.5Al-0.3C steel via in situ synchrotron X-ray diffraction during a tensile test, Materials 10 (2017), https://doi.org/10.3390/ma10101129.
[42] T. Ungár, Microstructural parameters from X-ray diffraction peak broadening, Scripta Mater. 51 (2004) 777–781, https://doi.org/10.1016/j.scriptamat.2004.05.007.
[43] N.C. Popa, The (hkl) dependence of diffraction-line broadening caused by strain and size for all laue groups in Rietveld refinement, J. Appl. Crystallogr. 31 (1998) 176–180, https://doi.org/10.1107/S0021889897009795.
[44] G.K. Williamson, R.E. Smallman III., Dislocation densities in some annealed and cold-worked metals from measurements on the X-ray debye-scherrer spectrum, Phil. Mag. 1 (1956) 34–46, https://doi.org/10.1080/14786435608238074.
[45] Y. Lü, D.A. Molodov, G. Gottstein, Recrystallization kinetics and microstructure evolution during annealing of a cold-rolled Fe–Mn–C alloy, Acta Mater. 59 (2011) 3229–3243, https://doi.org/10.1016/j.actamat.2011.01.063.
[46] C. Haase, T. Ingendahl, O. Güvenç, M. Bambach, W. Bleck, D.A. Molodov, L. A. Barrales-Mora, On the applicability of recovery-annealed Twinning-Induced Plasticity steels: potential and limitations, Materials Science and Engineering: A 649 (2016) 74–84, https://doi.org/10.1016/j.msea.2015.09.096.

[47] Z.C. Yanushkevich, D.A. Molodov, A.N. Belyakov, R.O. Kaibyshev, Recrystallization kinetics of an austenitic high-manganese steel subjected to severe plastic deformation, Russ. Metall. 2016 (2016) 812–819, https://doi.org/10.1134/S0036029516090184.
[48] O. Bouaziz, D. Barbier, Benefits of recovery and partial recrystallization of nano-twinned austenitic steels, Adv. Eng. Mater. 11 (2013) 976–979, https://doi.org/10.1002/adem.201300045.
[49] K.-T. Park, Y.-S. Kim, J.G. Lee, D.H. Shin, Thermal stability and mechanical properties of ultrafine grained low carbon steel, Materials Science and Engineering: A 293 (2000) 165–172, https://doi.org/10.1016/S0921-5093(00)01220-X.
[50] F.K. Yan, N.R. Tao, K. Lu, Tensile ductility of nanotwinned austenitic grains in an austenitic steel, Scripta Mater. 84–85 (2014) 31–34, https://doi.org/10.1016/j.scriptamat.2014.04.008.
[51] S.-J. Lee, J. Kim, S.N. Kane, B.C.D. Cooman, On the origin of dynamic strain aging in twinning-induced plasticity steels, Acta Mater. 59 (2011) 6809–6819, https://doi.org/10.1016/j.actamat.2011.07.040.
[52] F. Maresca, V.G. Kouznetsova, M. Geers, W.A. Curtin, Contribution of austenite-martensite transformation to deformability of advanced high strength steels: from atomistic mechanisms to microstructural response, Acta Mater. 156 (2018) 463–478, https://doi.org/10.1016/j.actamat.2018.06.028.
[53] J.P.M. Hoefnagels, C.C. Tasan, F. Maresca, F.J. Peters, V.G. Kouznetsova, Retardation of plastic instability via damage-enabled microstrain delocalization, J. Mater. Sci. 50 (2015) 6882–6897, https://doi.org/10.1007/s10853-015-9164-0.
[54] T. Wu, R. Wu, B. Liu, W. Liang, D. Ke, Microstructural and mechanical properties of ultra-high-strength dual-phase steel produced by ultra-fast cooling, Mater. Sci. Technol. 36 (2020) 843–851, https://doi.org/10.1080/02670836.2020.1744834.